Search for decays of neutral beauty mesons into four muons

LHCb Collaboration

Link to publication in University of Groningen/UMCG research database

Search for decays of neutral beauty mesons into four muons

The LHCb collaboration

E-mail: tobias.tekampe@cern.ch

ABSTRACT: A search for the non-resonant decays $B_s^0 \to \mu^+\mu^-\mu^+\mu^-$ and $B^0 \to \mu^+\mu^-\mu^+\mu^-$ is presented. The measurement is performed using the full Run 1 data set collected in proton-proton collisions by the LHCb experiment at the LHC. The data correspond to integrated luminosities of 1 and $2\,\mathrm{fb}^{-1}$ collected at centre-of-mass energies of 7 and $8\,\mathrm{TeV}$, respectively. No signal is observed and upper limits on the branching fractions of the non-resonant decays at 95% confidence level are determined to be

$$\mathcal{B}(B_s^0 \to \mu^+\mu^-\mu^+\mu^-) < 2.5 \times 10^{-9},$$
$$\mathcal{B}(B^0 \to \mu^+\mu^-\mu^+\mu^-) < 6.9 \times 10^{-10}.$$

Contents

1 Introduction

The rare decays $B^0_{(s)} \to \mu^+\mu^-\mu^+\mu^-$ proceed through $b \to d(s)$ flavour-changing neutral-current processes, which are strongly suppressed in the Standard Model (SM).[1] In the main non-resonant SM amplitude, one muon pair is produced via amplitudes described by electroweak loop diagrams and the other is created by a virtual photon as shown in figure 1(a). The branching fraction of the non-resonant $B^0_s \to \mu^+\mu^-\mu^+\mu^-$ decay is expected to be 3.5×10^{-11} [1].

Theories extending the SM can significantly enhance the $B^0_{(s)} \to \mu^+\mu^-\mu^+\mu^-$ decay rate by contributions of new particles. For example, in minimal supersymmetric models (MSSM), the decay can proceed via new scalar S and pseudoscalar P sgoldstino particles, which both decay into a dimuon final state as shown in figure 1(b). There are two types of couplings between sgoldstinos and SM fermions. Type-I couplings describe interactions between a sgoldstino and two fermions, where the coupling strength is proportional to the fermion mass. Type-II couplings describe a four-particle vertex, where a scalar and a pseudoscalar sgoldstino interact with two fermions. Branching fractions up to $\mathcal{B}(B^0_s \to SP) \approx 10^{-4}$ and $\mathcal{B}(B^0 \to SP) \approx 10^{-7}$ are possible [2]. Sgoldstinos can decay into a pair of photons or a pair of charged leptons [3]. In this analysis the muonic decay is considered, as the coupling to electrons is smaller and the large τ-lepton mass limits the available phase space. The branching fractions of the sgoldstino decays strongly depend on the model parameters such as the sgoldstino mass and the supersymmetry breaking scale. In the search for $\Sigma^+ \to p\mu^+\mu^-$ decays the HyperCP collaboration found an excess of events,

---

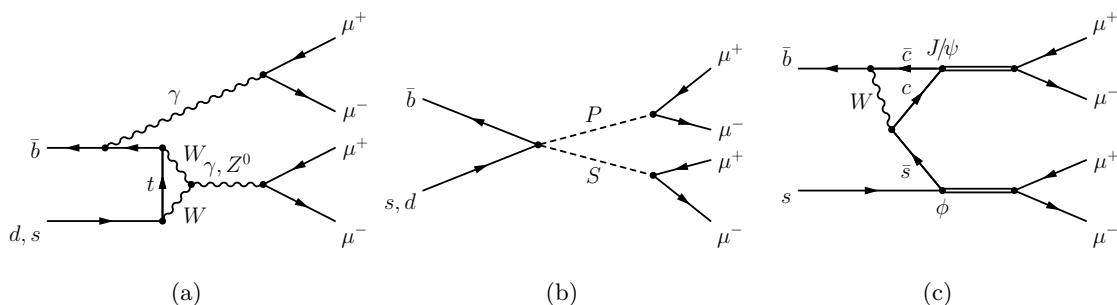[1]The inclusion of charge-conjugate processes is implied throughout.

Figure 1. Feynman diagrams for (a) the non-resonant $B_{(s)}^0 \to \mu^+\mu^-\mu^+\mu^-$ decay, (b) a supersymmetric $B_{(s)}^0 \to S(\to \mu^+\mu^-)P(\to \mu^+\mu^-)$ decay and (c) the resonant $B_s^0 \to J/\psi(\to \mu^+\mu^-)\phi(\to \mu^+\mu^-)$ decay (see text).

which is consistent with the decay $\Sigma^+ \to Pp$ with $P \to \mu^+\mu^-$ and a pseudoscalar mass of $m(P) = 214.3 \pm 0.5 \,\mathrm{MeV}$ [4].

So far only limits on the SM and MSSM branching fractions at 95% confidence level have been measured by LHCb based on the data recorded in 2011 [5] to be

$$\mathcal{B}(B_s^0 \to \mu^+\mu^-\mu^+\mu^-) < 1.6 \times 10^{-8},$$
$$\mathcal{B}(B^0 \to \mu^+\mu^-\mu^+\mu^-) < 6.6 \times 10^{-9},$$
$$\mathcal{B}(B_s^0 \to S(\to \mu^+\mu^-)P(\to \mu^+\mu^-)) < 1.6 \times 10^{-8},$$
$$\mathcal{B}(B^0 \to S(\to \mu^+\mu^-)P(\to \mu^+\mu^-)) < 6.3 \times 10^{-9}.$$

These limits are based on assumed sgoldstino masses of $m(S) = 2.5 \,\mathrm{GeV}/c^2$, which is approximately the central value of the allowed mass range, and $m(P) = 214.3 \,\mathrm{MeV}/c^2$.

The dominant SM decays of neutral B mesons into four muons proceed through resonances like ϕ, J/ψ and $\psi(2S)$. The most frequent of these decays is $B_s^0 \to J/\psi\,\phi$, where both the J/ψ and the ϕ mesons decay into a pair of muons, as shown in figure 1(c). In the following, this decay is referred to as the resonant decay mode and treated as a background. From the product of the measured branching fractions of the underlying decays $\mathcal{B}(B_s^0 \to J/\psi\,\phi)$, $\mathcal{B}(J/\psi \to \mu^+\mu^-)$, and $\mathcal{B}(\phi \to \mu^+\mu^-)$ [6] its branching fraction is calculated to be $(1.83 \pm 0.18) \times 10^{-8}$.

In this paper a search for the non-resonant SM process, and for the MSSM-induced $B_{(s)}^0 \to \mu^+\mu^-\mu^+\mu^-$ decays is presented, using pp collision data recorded by the LHCb detector during LHC Run 1. Potentially contributing sgoldstinos are assumed to be short lived, such that they do not form a displaced vertex. The analysed data correspond to integrated luminosities of 1 and $2\,\mathrm{fb}^{-1}$ collected at centre-of-mass energies of 7 and $8\,\mathrm{TeV}$, respectively. The branching fraction is measured relative to the decay $B^+ \to J/\psi(\to \mu^+\mu^-)K^+$, which gives a clean signal with a precisely measured branching fraction [6]. This yields a significant improvement compared to the previous measurement, where the use of the $B^0 \to J/\psi\,K^{*0}$ decay as normalisation mode resulted in a large systematic uncertainty originating from the S-wave fraction and the less precisely measured branching fraction. The advantage of normalising to a well-known B meson decay is that dominant systematic uncertainties originating mainly from the $b\bar{b}$ cross-section cancel in the ratio.

2 Detector and simulation

The LHCb detector [7, 8] is a single-arm forward spectrometer covering the pseudorapidity range $2 < \eta < 5$, designed for the study of particles containing b or c quarks. The detector includes a high-precision tracking system consisting of a silicon-strip vertex detector surrounding the pp interaction region, a large-area silicon-strip detector located upstream of a dipole magnet with a bending power of about $4\,\mathrm{Tm}$, and three stations of silicon-strip detectors and straw drift tubes placed downstream of the magnet. The tracking system provides a measurement of momentum, p, of charged particles with a relative uncertainty that varies from 0.5% at low momentum to 1.0% at $200\,\mathrm{GeV}/c$. The minimum distance of a track to a primary vertex (PV), the impact parameter, is measured with a resolution of $(15 + 29/p_{\mathrm{T}})\,\mu\mathrm{m}$, where p_{T} is the component of the momentum transverse to the beam, in GeV/c. Different types of charged hadrons are distinguished using information from two ring-imaging Cherenkov (RICH) detectors. Photons, electrons and hadrons are identified by a calorimeter system consisting of scintillating-pad and preshower detectors, an electromagnetic calorimeter and a hadronic calorimeter. Muons are identified by a system composed of alternating layers of iron and multiwire proportional chambers.

In the simulation, pp collisions are generated using Pythia [9, 10] with a specific LHCb configuration [11]. Decays of hadronic particles are described by EvtGen [12], in which final-state radiation is generated using Photos [13]. The interaction of the generated particles with the detector, and its response, are implemented using the Geant4 toolkit [14, 15] as described in ref. [16].

3 Event selection

The online event selection is performed by a trigger, which consists of a hardware stage, based on information from the calorimeter and muon systems, followed by a software stage, which applies a full event reconstruction. In this analysis candidate events are first required to pass the hardware trigger, which for $7\,\mathrm{TeV}$ ($8\,\mathrm{TeV}$) data selects events with at least one muon with a transverse momentum of $p_{\mathrm{T}} > 1.48\,\mathrm{GeV}/c$ ($p_{\mathrm{T}} > 1.76\,\mathrm{GeV}/c$) or at least one pair of muons with the product of the transverse momenta larger than $(1.296)^2\ \mathrm{GeV}^2/c^2$ $((1.6)^2\ \mathrm{GeV}^2/c^2)$. In the subsequent software trigger, at least one of the final-state particles is required to have $p_{\mathrm{T}} > 1\,\mathrm{GeV}/c$ and an impact parameter larger than $100\,\mu\mathrm{m}$ with respect to all PVs in the event.

In the offline selection, the $B^0_{(s)}$ decay vertex is constructed from four good quality muon candidates that form a common vertex and have a total charge of zero. The vertex is required to be significantly displaced from any PV. Among the four final-state muons, there are four possible dimuon combinations with zero charge. In all four combinations, the mass windows corresponding to the ϕ (950–1090 MeV/c^2), J/ψ (3000–3200 MeV/c^2) and $\psi(2S)$ (3600–3800 MeV/c^2) resonances are vetoed. This efficiently suppresses any background from any of the three mentioned resonances to a negligible level. Contributions of other charmonium states are found to be negligible.

The MatrixNet (MN) [17], a multivariate classifier based on a Boosted Decision Tree [18, 19], is applied in order to remove combinatorial background, where a candidate $B_{(s)}^0$ vertex is constructed from four muons that do not originate from a single B meson decay. The input variables are the following properties of the $B_{(s)}^0$ candidate: the decay time, the vertex quality, the momentum and transverse momentum, the cosine of the direction angle (DIRA), and the smallest impact parameter chisquare (χ_{IP}^2) with respect to any PV, where χ_{IP}^2 is defined as the difference between the vertex-fit χ^2 of a PV reconstructed with and without the $B_{(s)}^0$ candidate. The DIRA is defined as the angle between the momentum of the reconstructed $B_{(s)}^0$ candidate and the vector from the PV with the smallest χ_{IP}^2 to the $B_{(s)}^0$ decay vertex. As training samples, simulated $B_s^0 \to \mu^+\mu^-\mu^+\mu^-$ and $B^0 \to \mu^+\mu^-\mu^+\mu^-$ events, generated with a uniform probability across the decay phase space, are used as a signal proxy. Before training, the signal simulation is weighted to correct for known discrepancies between data and simulation as described later. The background sample is taken from the far and the near sidebands in data as defined in table 1. In order to verify that the classification of each event is unbiased, 10-fold cross-validation [20] is employed.

Background arising from misidentifying one or more particles is suppressed by applying particle identification (PID) requirements. Information from the RICH system, the calorimeters and the muon system is used to calculate the difference in log-likelihood between the hypothesis of a final-state particle being a pion or a muon, $\mathrm{DLL}_{\mu\pi}$.

Events in the signal region are not examined until the analysis is finalised. Events outside the signal region are split into the far sidebands, used to calculate the expected background yield, and the near sidebands, used to optimise the cuts on the MN response and the minimum $\mathrm{DLL}_{\mu\pi}$ values of the four muon candidates in the final state. The optimization of the cuts is performed on a two-dimensional grid maximising the figure of merit [21]

$$\mathrm{FoM} = \frac{\varepsilon_{\mathrm{signal}}}{\sigma/2 + \sqrt{N_{\mathrm{bkg}}^{\mathrm{expected}} \times \varepsilon_{\mathrm{bkg}}}}.$$

The intended significance in terms of standard deviations (σ) is set to three. Very similar selection criteria are found when using five. The expected background yield before applying the MN and PID selection, $N_{\mathrm{bkg}}^{\mathrm{expected}}$, is determined from a fit to the events in the near sidebands using an exponential function. For each grid point the background efficiency, $\varepsilon_{\mathrm{bkg}}$, is measured using events from the near sidebands. The signal efficiency, $\varepsilon_{\mathrm{signal}}$, is measured for each grid point using simulated $B_{(s)}^0 \to \mu^+\mu^-\mu^+\mu^-$ decays. Lacking a model for non-resonant $B_{(s)}^0 \to \mu^+\mu^-\mu^+\mu^-$ simulation, the selection of the preceding measurement was developed on $B_s^0 \to J/\psi\,(\to \mu^+\mu^-)\phi(\to \mu^+\mu^-)$ data. Now that a suitable simulation model is available, significant improvements in terms of signal efficiency and background rejection are made by employing a multivariate classifier and being able to measure the selection efficiency from simulation.

4 Selection efficiencies and systematic uncertainties

The optimal working point corresponds to signal efficiencies of $(0.580 \pm 0.003)\%$ and

	Mass interval (MeV/c^2)
Near sidebands	$[5020, 5220]$ and $[5426, 5626]$
Far sidebands	$[4360, 5020]$ and $[5626, 6360]$
Signal region	$[m(B^0) - 60, m(B^0_s) + 60]$
B^0_s search region	$[m(B^0_s) - 40, m(B^0_s) + 40]$
B^0 search region	$[m(B^0) - 40, m(B^0) + 40]$

Table 1. Definitions of intervals in the B^0 and B^0_s reconstructed invariant mass distributions.

$(0.568 \pm 0.003)\%$ for the $B^0_s \to \mu^+\mu^-\mu^+\mu^-$ and $B^0 \to \mu^+\mu^-\mu^+\mu^-$ decay modes, respectively. Sources of peaking background such as $B^0 \to K^{*0}\mu^+\mu^-$, in which the kaon and the pion originating from the K^* decay are misidentified as muons, are reduced to a negligible level by the optimised selection. The efficiencies for the MSSM processes are measured using simulated samples of the $B^0_{(s)} \to S(\to \mu^+\mu^-)P(\to \mu^+\mu^-)$ decays, where the $B^0_{(s)}$ meson decays into a pseudoscalar sgoldstino with a mass of $214.3\,\mathrm{MeV}/c^2$ [4] and a scalar sgoldstino with a mass of $2.5\,\mathrm{GeV}/c^2$. Both the P and S particles are simulated with a decay width of $\Gamma = 0.1\,\mathrm{MeV}/c^2$, which corresponds to a prompt decay. The measured efficiencies are the same for the B^0_s and the B^0 decays and amount to $(0.648 \pm 0.003)\%$. The difference between the SM and the MSSM efficiencies originates from the fact that in the case of the decay proceeding via P and S sgoldstinos, the decay products are more likely to be within the acceptance of the LHCb detector. In order to test the dependence of the measured $B^0_{(s)} \to S(\to \mu^+\mu^-)P(\to \mu^+\mu^-)$ branching fractions on the mass of the scalar sgoldstino, the selection efficiency is measured in bins of dimuon invariant mass while requiring the corresponding other dimuon mass to be between 200 and $950\,\mathrm{MeV}/c^2$. An efficiency variation of $\mathcal{O}(20\%)$ is observed.

The selection applied to the normalisation mode $B^+ \to J/\psi(\to \mu^+\mu^-)K^+$ differs from that applied to the signal modes in the PID criteria and that no multivariate analysis technique is applied. The total efficiency is $(1.495 \pm 0.006)\%$. The uncertainties on the efficiencies are driven by the limited number of simulated events and are treated as systematic uncertainties of 0.4–0.5%.

The total efficiency is calculated as the product of the efficiencies of the different stages of the selection. As an alternative to the trigger efficiency calculated on simulation, the value is calculated on $B^+ \to J/\psi(\to \mu^+\mu^-)K^+$ data [22] and a systematic uncertainty of 3% is assigned corresponding to the relative difference. The efficiency of the MN classifier to select the more frequent decay $B^0_s \to J/\psi(\to \mu^+\mu^-)\phi(\to K^+K^-)$ is compared between data and simulation. The relative difference of 0.3% is assigned as a systematic uncertainty. Another source of systematic uncertainty arises from the track finding efficiency. Again, values obtained from data [23] and simulation are compared and the deviation is treated as a correction factor for the efficiency, while the uncertainty on the deviation, 1.7%, is assigned as a systematic uncertainty.

In general the agreement in the observables used in the selection between data and simulation is very good, although there are some distributions that are known to deviate.

Therefore, the gradient boosting reweighting technique [24] is used to calculate weights that correct for differences between data and simulation in $B_s^0 \to J/\psi(\to \mu^+\mu^-)\phi(\to K^+K^-)$. The weighting is performed in the track multiplicity, the B transverse momentum, the χ^2 of the decay vertex fit and the χ^2_{IP}. The first two are chosen because they are correlated with the PID variables and the latter two dominate the feature ranking obtained from the MN training. These weights are applied to the $B_{(s)}^0 \to \mu^+\mu^-\mu^+\mu^-$ and $B^+ \to J/\psi(\to \mu^+\mu^-)K^+$ simulation samples, and are used to calculate the MN and the PID efficiencies. In order to account for inaccuracies of this method resulting from the kinematic and topological differences between the decay modes, systematic uncertainties of 3.6% are assigned based on the difference of the MN efficiency on $B_{(s)}^0 \to \mu^+\mu^-\mu^+\mu^-$ and $B_s^0 \to J/\psi(\to \mu^+\mu^-)\phi(\to K^+K^-)$. For the $B^+ \to J/\psi(\to \mu^+\mu^-)K^+$ decay mode, the efficiencies are measured with and without weights and the observed difference of 2.3% is assigned as systematic uncertainty.

In order to determine accurate efficiencies of the applied PID requirements, calibration samples of muons from $J/\psi \to \mu^+\mu^-$ and $\phi \to \mu^+\mu^-$ decays and of kaons from $D^{*+} \to D^0(\to K^-\pi^+)\pi^+$ decays are used. The relative frequency for kaons and muons to pass the PID criteria is calculated in bins of track multiplicity, particle momentum and pseudorapidity. Different binning schemes are tested and the observed differences in the efficiencies of 1% for $B^+ \to J/\psi(\to \mu^+\mu^-)K^+$ and 0.5% for $B_{(s)}^0 \to \mu^+\mu^-\mu^+\mu^-$ are assigned as systematic uncertainties. Additionally, 3% of the simulated $B_{(s)}^0 \to \mu^+\mu^-\mu^+\mu^-$ decays contain muons with low transverse momentum outside the kinematic region covered by the calibration data. This fraction is assigned as a systematic uncertainty. Candidates that have a reconstructed invariant mass within $\pm 40\,\mathrm{MeV}/c^2$ around the known $B_{(s)}^0$ mass, which corresponds to $\pm 2\sigma$ of the mass resolution, are treated as signal candidates. The accuracy of the efficiency of this cut is evaluated on $B_s^0 \to J/\psi(\to \mu^+\mu^-)\phi(\to K^+K^-)$ data. A systematic uncertainty of 0.5% corresponding to the relative difference of the efficiency measured on data and simulation is assigned. Systematic uncertainties of 0.9% and 0.5% in the case of $B_{(s)}^0 \to \mu^+\mu^-\mu^+\mu^-$ and $B^+ \to J/\psi(\to \mu^+\mu^-)K^+$ originate from the imperfections of the efficiency of the event reconstruction due to soft photon radiation and 0.6% from mismatching of track segments between different tracking stations in the detector, which is measured using simulated events. All relevant sources of systematic uncertainty along with the total values are summarised in table 2. The most significant improvements with regard to the preceding measurement are the larger available data sample, and the choice of the $B^+ \to J/\psi(\to \mu^+\mu^-)K^+$ decay as normalisation mode, which has the advantage of a precisely measured branching fraction and the absence of an additional systematic uncertainty originating from the S-wave correction.

5   Normalisation

The $B^+ \to J/\psi(\to \mu^+\mu^-)K^+$ signal yield is determined by performing an unbinned extended maximum likelihood fit to the $K^+\mu^+\mu^-$ invariant mass distribution. In this fit the J/ψ mass is constrained [25] to the world average [6]. The normalisation yield is found to be $N(B^+ \to J/\psi(\to \mu^+\mu^-)K^+) = 687890 \pm 920$. The $J/\psi K^+$ mass spectrum along

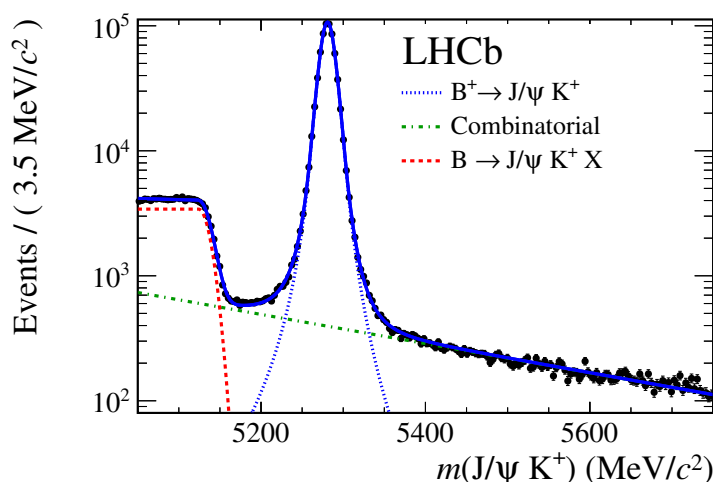**Figure 2**. Fit to the $B^+ \to J/\psi\,(\to \mu^+\mu^-)K^+$ invariant mass distribution. The signal contribution is modelled by a Hypatia2 [26] function (blue dotted line), the combinatorial background by an exponential function (green dash-dotted line). Partially reconstructed decays, such as $B^0 \to J/\psi\,K^{*0}$ where one pion is not reconstructed, are modelled by a Gaussian function with an exponential tail towards the lower mass side (red dashed line). Data are shown by black dots.

with the fit result is shown in figure 2. A systematic uncertainty of 0.3% is assigned to the determined $B^+ \to J/\psi\,(\to \mu^+\mu^-)K^+$ yield by using an alternative fit model and performing a binned extended maximum likelihood fit.

The $B^0_{(s)} \to \mu^+\mu^-\mu^+\mu^-$ branching fraction is calculated as

$$\mathcal{B}(B^0_{(s)} \to \mu^+\mu^-\mu^+\mu^-) = N(B^0_{(s)} \to \mu^+\mu^-\mu^+\mu^-) \times \eta_{d,s},$$

with

$$\eta_{d,s} = \frac{\varepsilon(B^+ \to J/\psi\,(\to \mu^+\mu^-)K^+) \times \mathcal{B}(B^+ \to J/\psi\,(\to \mu^+\mu^-)K^+)}{\varepsilon(B^0_{(s)} \to \mu^+\mu^-\mu^+\mu^-) \times N(B^+ \to J/\psi\,(\to \mu^+\mu^-)K^+)} \times \frac{f_u}{f_{d,s}},$$

where $N(B^+ \to J/\psi\,(\to \mu^+\mu^-)K^+)$ and $N(B^0_{(s)} \to \mu^+\mu^-\mu^+\mu^-)$ are the observed yields of the normalisation and the signal channel, respectively. The ratio between the production rates of B^0_s and B^0 was measured by LHCb to be $f_s/f_d = 0.259 \pm 0.015$ [27]. The measurement was performed using pp collision data at $\sqrt{s} = 7$ TeV, but found to be stable between $\sqrt{s} = 7$ TeV and 8 TeV by a previous LHCb measurement [28]. The ratio between the B^+ and B^0 production rates is assumed to be unity. As a consequence f_s/f_u is equal to f_s/f_d.

The single event sensitivities, $\eta_{d,s}$, amount

$$\eta_s^{\rm SM} = (8.65 \pm 0.80) \times 10^{-10},$$
$$\eta_d^{\rm SM} = (2.29 \pm 0.16) \times 10^{-10},$$
$$\eta_s^{\rm MSSM} = (7.75 \pm 0.72) \times 10^{-10},$$
$$\eta_d^{\rm MSSM} = (2.01 \pm 0.14) \times 10^{-10},$$

for the B_s^0 and the B^0 decay modes in the SM and in the MSSM scenario. Here, the uncertainties are the combined values of the statistical uncertainty on the $B^+ \to J/\psi(\to \mu^+\mu^-)K^+$ yield and the systematic uncertainty. In the case of η_s the systematic uncertainty is dominated by the ratio of f_u/f_s and in the case of η_d by the weighting procedure applied to correct for the difference between data and simulation.

The individual sources of systematic uncertainties given in table 2 are assumed to be uncorrelated and are combined quadratically. The total systematic uncertainty is 9.2% for the B_s^0 decay and 7.2% for the B^0 decay. These values are small compared to the statistical uncertainty on the expected number of background events in the B^0 and B_s^0 search regions. The whole analysis strategy is cross-checked by measuring the $B_s^0 \to J/\psi(\to \mu^+\mu^-)\phi(\to \mu^+\mu^-)$ branching fraction. The obtained value has a precision of 20% and is compatible with the product of the branching fractions of the underlying decays taken from ref. [6].

The number of expected background events is determined by fitting an exponential function to the far sidebands of $m(\mu^+\mu^-\mu^+\mu^-)$. Extrapolating and integrating the fitted function in $\pm 40 \, \mathrm{MeV}/c^2$ wide windows around the $B_{(s)}^0$ meson masses yields the number of expected background events,

$$N_{\mathrm{bkg}}^{\mathrm{expected}}(B^0) = 0.55^{+0.24}_{-0.19}\,(\mathrm{stat}) \pm 0.20\,(\mathrm{syst}) \quad \text{and}$$
$$N_{\mathrm{bkg}}^{\mathrm{expected}}(B_s^0) = 0.47^{+0.23}_{-0.18}\,(\mathrm{stat}) \pm 0.18\,(\mathrm{syst}).$$

The statistical uncertainty is the combination of the Poissonian uncertainty originating from the limited size of the data sample and the uncertainty on the fit parameters. As an alternative fit model a second-order polynomial is used and the difference between these background expectations is assigned as a systematic uncertainty.

6 Results

The final distribution of the reconstructed mass of the four muon system is shown in figure 3. No candidates are observed in either the B^0 or the B_s^0 search region, which is consistent with the expected background yield.

The Hybrid CLs procedure [29–31], with log-normal priors to account for uncertainties of both background and efficiency estimations, is used to convert the observations into upper limits on the corresponding branching fractions. The exclusion at 95% confidence level assuming the SM single event sensitivities is shown in figure 4. The result for the corresponding MSSM values is presented in figure 5. The limits on the branching fractions of the B_s^0 and B^0 decays are anti-correlated. Replacing the log-normal priors by gamma distributions yields the same results.

Assuming negligible cross-feed between the B_s^0 and the B^0 search regions, the observed upper limits on the branching fractions at 95% confidence level are found to be

$$\mathcal{B}(B_s^0 \to \mu^+\mu^-\mu^+\mu^-) < 2.5 \times 10^{-9},$$
$$\mathcal{B}(B^0 \to \mu^+\mu^-\mu^+\mu^-) < 6.9 \times 10^{-10},$$
$$\mathcal{B}(B_s^0 \to S(\to \mu^+\mu^-)P(\to \mu^+\mu^-)) < 2.2 \times 10^{-9},$$
$$\mathcal{B}(B^0 \to S(\to \mu^+\mu^-)P(\to \mu^+\mu^-)) < 6.0 \times 10^{-10}.$$

Source	Value [%]
Selection efficiency	$0.4 - 0.5$
Trigger efficiency	3.0
MN efficiency	0.3
Track finding efficiency	1.7
Weighting $B^0_{(s)} \to \mu^+\mu^-\mu^+\mu^-$	3.6
Weighting $B^+ \to J/\psi(\to \mu^+\mu^-)K^+$	2.3
PID binning $B^+ \to J/\psi(\to \mu^+\mu^-)K^+$	1.0
PID binning $B^0_{(s)} \to \mu^+\mu^-\mu^+\mu^-$	0.5
Kinematic coverage of PID calibration data	3.0
$\pm 40\,\mathrm{MeV}/c^2$ search region efficiency	0.5
Soft photon radiation $B^0_{(s)} \to \mu^+\mu^-\mu^+\mu^-$	0.9
Soft photon radiation $B^+ \to J/\psi(\to \mu^+\mu^-)K^+$	0.5
Track segments mismatching	0.6
Normalisation fit	0.3
f_u/f_s	5.8
$\mathcal{B}(B^+ \to J/\psi K^+)$	3.0
$\mathcal{B}(J/\psi \to \mu^+\mu^-)$	0.1
Combined η_s SM	9.2
Combined η_d SM	7.2
Combined η_s MSSM	9.2
Combined η_d MSSM	7.2

Table 2. Summary of systematic uncertainties affecting the single event sensitivities along with the total systematic uncertainty calculated by adding up the individual components in quadrature. The dominating uncertainty arising from f_u/f_s only contributes to η_s. The uncertainty of the stated selection efficiencies arising from the limited number of simulated events is 0.5% for $B^0 \to \mu^+\mu^-\mu^+\mu^-$ and 0.4% for all other considered decay modes.

7 Conclusion

In summary, a search for non-resonant $B^0_{(s)} \to \mu^+\mu^-\mu^+\mu^-$ decays has been presented. In addition, the sensitivity to a specific MSSM scenario has been probed. The applied selection focuses on finding four muon tracks that form a common vertex. For the SM scenario and the MSSM decay through short-lived scalar and pseudoscalar new particles, the limits set by the previous measurement performed by LHCb on a subset of the present data, are improved by a factor of 6.4 (7.3) for the SM (MSSM) mode in the case of the B^0_s decay and by a factor of 9.5 (10.5) in the case of the B^0 decay.
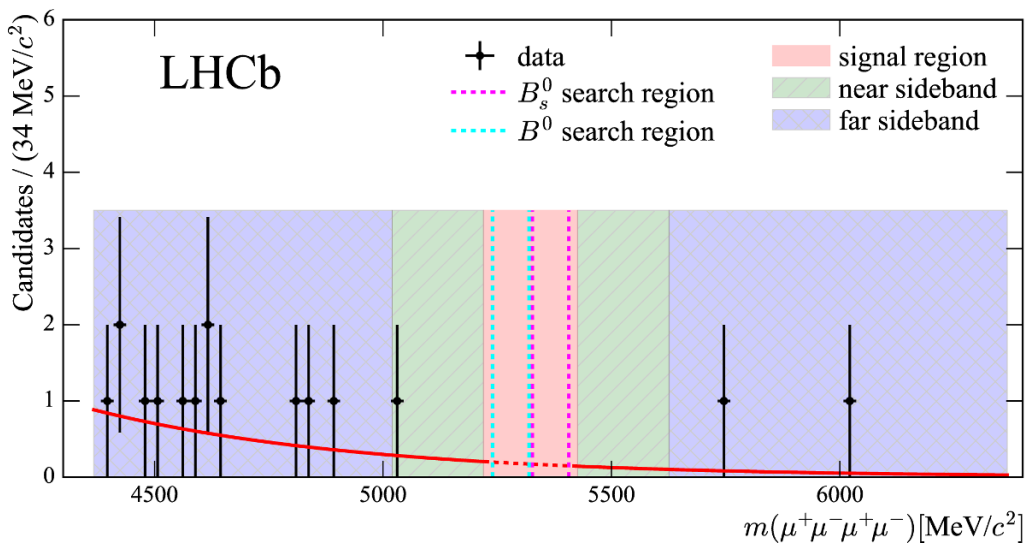
Figure 3. Mass distribution of selected $B^0_{(s)} \to \mu^+\mu^-\mu^+\mu^-$ events observed in $3\,\mathrm{fb}^{-1}$ of data in all considered B mass regions. Background (red line) is modelled by an exponential function. Signal subregions for B^0 and B^0_s searches are also shown. The error bars on the individual points with n entries are $\pm\sqrt{n}$.
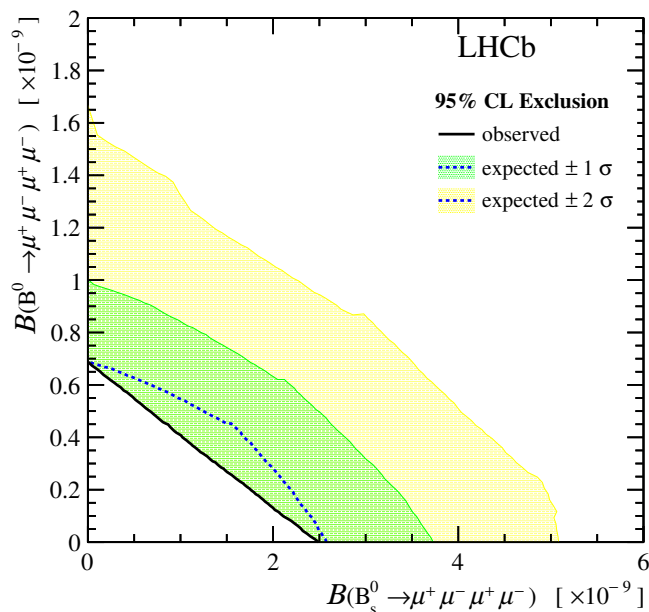
Figure 4. Expected and observed 95% CL exclusion in $\mathcal{B}(B^0 \to \mu^+\mu^-\mu^+\mu^-)$ vs. $\mathcal{B}(B^0_s \to \mu^+\mu^-\mu^+\mu^-)$ parameters plane.

Acknowledgments
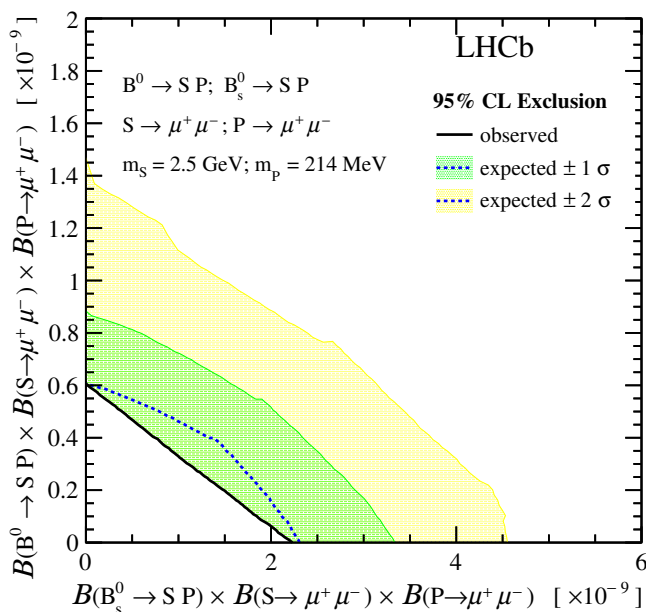
Figure 5. Expected and observed 95% CL exclusion in $\mathcal{B}(B^0 \to S(\to \mu^+\mu^-)P(\to \mu^+\mu^-))$ vs. $\mathcal{B}(B^0_s \to S(\to \mu^+\mu^-)P(\to \mu^+\mu^-))$ parameters plane with scalar and pseudoscalar S and P as described in section 3.

References

[1] Y. Dincer and L.M. Sehgal, *Electroweak effects in the double Dalitz decay $B_s \to \ell^+\ell^-\ell'^+\ell'^-$*, *Phys. Lett.* **B 556** (2003) 169 [hep-ph/0301056] [iNSPIRE].

[2] S.V. Demidov and D.S. Gorbunov, *Flavor violating processes with sgoldstino pair production*, *Phys. Rev.* **D 85** (2012) 077701 [`arXiv:1112.5230`] [ɪɴSPIRE].

[3] S.V. Demidov and D.S. Gorbunov, *More about sgoldstino interpretation of HyperCP events*, *JETP Lett.* **84** (2007) 479 [`hep-ph/0610066`] [ɪɴSPIRE].

[4] HʏᴘᴇʀCP collaboration, H. Park et al., *Evidence for the decay* $\Sigma^+ \to p\mu^+\mu^-$, *Phys. Rev. Lett.* **94** (2005) 021801 [`hep-ex/0501014`] [ɪɴSPIRE].

[5] LHCb collaboration, *Search for rare* $B^0_{(s)} \to \mu^+\mu^-\mu^+\mu^-$ *decays*, *Phys. Rev. Lett.* **110** (2013) 211801 [`arXiv:1303.1092`] [ɪɴSPIRE].

[6] Pᴀʀᴛɪᴄʟᴇ Dᴀᴛᴀ Gʀᴏᴜᴘ collaboration, C. Patrignani et al., *Review of particle physics*, *Chin. Phys.* **C 40** (2016) 100001 [ɪɴSPIRE].

[7] LHCb collaboration, *The LHCb detector at the LHC*, 2008 *JINST* **3** S08005 [ɪɴSPIRE].

[8] LHCb collaboration, *LHCb detector performance*, *Int. J. Mod. Phys.* **A 30** (2015) 1530022 [`arXiv:1412.6352`] [ɪɴSPIRE].

[9] T. Sjöstrand, S. Mrenna and P.Z. Skands, *PYTHIA 6.4 physics and manual*, *JHEP* **05** (2006) 026 [`hep-ph/0603175`] [ɪɴSPIRE].

[10] T. Sjöstrand, S. Mrenna and P.Z. Skands, *A brief introduction to PYTHIA 8.1*, *Comput. Phys. Commun.* **178** (2008) 852 [`arXiv:0710.3820`] [ɪɴSPIRE].

[11] LHCb collaboration, *Handling of the generation of primary events in Gauss, the LHCb simulation framework*, *J. Phys. Conf. Ser.* **331** (2011) 032047 [ɪɴSPIRE].

[12] D.J. Lange, *The EvtGen particle decay simulation package*, *Nucl. Instrum. Meth.* **A 462** (2001) 152 [ɪɴSPIRE].

[13] P. Golonka and Z. Was, *PHOTOS Monte Carlo: a precision tool for QED corrections in Z and W decays*, *Eur. Phys. J.* **C 45** (2006) 97 [`hep-ph/0506026`] [ɪɴSPIRE].

[14] Gᴇᴀɴᴛ4 collaboration, J. Allison et al., *GEANT4 developments and applications*, *IEEE Trans. Nucl. Sci.* **53** (2006) 270.

[15] GEANT4 collaboration, S. Agostinelli et al., *GEANT4: a simulation toolkit*, *Nucl. Instrum. Meth.* **A 506** (2003) 250 [ɪɴSPIRE].

[16] LHCb collaboration, *The LHCb simulation application, Gauss: design, evolution and experience*, *J. Phys. Conf. Ser.* **331** (2011) 032023 [ɪɴSPIRE].

[17] A. Gulin, I. Kuralenok and D. Pavlov, *Winning the transfer learning track of Yahoo!'s learning to rank challenge with YetiRank*, *JMLR Proc.* **14** (2011) 63.

[18] L. Breiman, J. H. Friedman, R. A. Olshen and C.J. Stone, *Classification and regression trees*, Wadsworth international group, Belmont U.S.A. (1984).

[19] R.E. Schapire and Y. Freund, *A decision-theoretic generalization of on-line learning and an application to boosting*, *J. Comput. Syst. Sci.* **55** (1997) 119.

[20] A. Blum, A. Kalai and J. Langford, *Beating the hold-out: bounds for k-fold and progressive cross-validation*, in the proceedings of the *Twelfth Annual Conference on Computational Learning Theory (COLT'99)*, July 7–9, New York, U.S.A. (1999).

[21] G. Punzi, *Sensitivity of searches for new signals and its optimization*, *eConf* **C 030908** (2003) MODT002 [`physics/0308063`] [ɪɴSPIRE].

[22] S. Tolk, J. Albrecht, F. Dettori and A. Pellegrino, *Data driven trigger efficiency determination at LHCb*, LHCb-PUB-2014-039 (2014).

[23] LHCb collaboration, *Measurement of the track reconstruction efficiency at LHCb*, 2015 *JINST* **10** P02007 [arXiv:1408.1251] [INSPIRE].

[24] A. Rogozhnikov, *Reweighting with boosted decision trees*, *J. Phys. Conf. Ser.* **762** (2016) 012036 [arXiv:1608.05806] [INSPIRE].

[25] W.D. Hulsbergen, *Decay chain fitting with a Kalman filter*, *Nucl. Instrum. Meth.* **A 552** (2005) 566 [physics/0503191] [INSPIRE].

[26] D. Martínez Santos and F. Dupertuis, *Mass distributions marginalized over per-event errors*, *Nucl. Instrum. Meth.* **A 764** (2014) 150 [arXiv:1312.5000] [INSPIRE].

[27] LHCb collaboration, *Updated average f_s/f_d b-hadron production fraction ratio for 7 TeV pp collisions*, LHCb-CONF-2013-011 (2013).

[28] LHCb collaboration, *Measurement of the $B_s^0 \to \mu^+\mu^-$ branching fraction and search for $B^0 \to \mu^+\mu^-$ decays at the LHCb experiment*, *Phys. Rev. Lett.* **111** (2013) 101805 [arXiv:1307.5024] [INSPIRE].

[29] R.D. Cousins and V.L. Highland, *Incorporating systematic uncertainties into an upper limit*, *Nucl. Instrum. Meth.* **A 320** (1992) 331 [INSPIRE].

[30] A.L. Read, *Presentation of search results: the CL(s) technique*, *J. Phys.* **G 28** (2002) 2693.

[31] T. Junk, *Confidence level computation for combining searches with small statistics*, *Nucl. Instrum. Meth.* **A 434** (1999) 435 [hep-ex/9902006] [INSPIRE].

The LHCb collaboration

R. Aaij[40], B. Adeva[39], M. Adinolfi[48], Z. Ajaltouni[5], S. Akar[6], J. Albrecht[10], F. Alessio[40],
M. Alexander[53], S. Ali[43], G. Alkhazov[31], P. Alvarez Cartelle[55], A.A. Alves Jr[59], S. Amato[2],
S. Amerio[23], Y. Amhis[7], L. An[41], L. Anderlini[18], G. Andreassi[41], M. Andreotti[17,g],
J.E. Andrews[60], R.B. Appleby[56], F. Archilli[43], P. d'Argent[12], J. Arnau Romeu[6], A. Artamonov[37],
M. Artuso[61], E. Aslanides[6], G. Auriemma[26], M. Baalouch[5], I. Babuschkin[56], S. Bachmann[12],
J.J. Back[50], A. Badalov[38], C. Baesso[62], S. Baker[55], W. Baldini[17], A. Baranov[35], R.J. Barlow[56],
C. Barschel[40], S. Barsuk[7], W. Barter[40], M. Baszczyk[27], V. Batozskaya[29], B. Batsukh[61],
V. Battista[41], A. Bay[41], L. Beaucourt[4], J. Beddow[53], F. Bedeschi[24], I. Bediaga[1], L.J. Bel[43],
V. Bellee[41], N. Belloli[21,i], K. Belous[37], I. Belyaev[32], E. Ben-Haim[8], G. Bencivenni[19], S. Benson[43],
J. Benton[48], A. Berezhnoy[33], R. Bernet[42], A. Bertolin[23], C. Betancourt[42], F. Betti[15],
M.-O. Bettler[40], M. van Beuzekom[43], Ia. Bezshyiko[42], S. Bifani[47], P. Billoir[8], T. Bird[56],
A. Birnkraut[10], A. Bitadze[56], A. Bizzeti[18,u], T. Blake[50], F. Blanc[41], J. Blouw[11,†], S. Blusk[61],
V. Bocci[26], T. Boettcher[58], A. Bondar[36,w], N. Bondar[31,40], W. Bonivento[16], I. Bordyuzhin[32],
A. Borgheresi[21,i], S. Borghi[56], M. Borisyak[35], M. Borsato[39], F. Bossu[7], M. Boubdir[9],
T.J.V. Bowcock[54], E. Bowen[42], C. Bozzi[17,40], S. Braun[12], M. Britsch[12], T. Britton[61],
J. Brodzicka[56], E. Buchanan[48], C. Burr[56], A. Bursche[2], J. Buytaert[40], S. Cadeddu[16],
R. Calabrese[17,g], M. Calvi[21,i], M. Calvo Gomez[38,m], A. Camboni[38], P. Campana[19],
D.H. Campora Perez[40], L. Capriotti[56], A. Carbone[15,e], G. Carboni[25,j], R. Cardinale[20,h],
A. Cardini[16], P. Carniti[21,i], L. Carson[52], K. Carvalho Akiba[2], G. Casse[54], L. Cassina[21,i],
L. Castillo Garcia[41], M. Cattaneo[40], Ch. Cauet[10], G. Cavallero[20], R. Cenci[24,t], D. Chamont[7],
M. Charles[8], Ph. Charpentier[40], G. Chatzikonstantinidis[47], M. Chefdeville[4], S. Chen[56],
S.-F. Cheung[57], V. Chobanova[39], M. Chrzaszcz[42,27], X. Cid Vidal[39], G. Ciezarek[43],
P.E.L. Clarke[52], M. Clemencic[40], H.V. Cliff[49], J. Closier[40], V. Coco[59], J. Cogan[6], E. Cogneras[5],
V. Cogoni[16,40,f], L. Cojocariu[30], G. Collazuol[23,o], P. Collins[40], A. Comerma-Montells[12],
A. Contu[40], A. Cook[48], G. Coombs[40], S. Coquereau[38], G. Corti[40], M. Corvo[17,g],
C.M. Costa Sobral[50], B. Couturier[40], G.A. Cowan[52], D.C. Craik[52], A. Crocombe[50],
M. Cruz Torres[62], S. Cunliffe[55], R. Currie[55], C. D'Ambrosio[40], F. Da Cunha Marinho[2],
E. Dall'Occo[43], J. Dalseno[48], P.N.Y. David[43], A. Davis[59], O. De Aguiar Francisco[2],
K. De Bruyn[6], S. De Capua[56], M. De Cian[12], J.M. De Miranda[1], L. De Paula[2], M. De Serio[14,d],
P. De Simone[19], C.-T. Dean[53], D. Decamp[4], M. Deckenhoff[10], L. Del Buono[8], M. Demmer[10],
A. Dendek[28], D. Derkach[35], O. Deschamps[5], F. Dettori[40], B. Dey[22], A. Di Canto[40], H. Dijkstra[40],
F. Dordei[40], M. Dorigo[41], A. Dosil Suárez[39], A. Dovbnya[45], K. Dreimanis[54], L. Dufour[43],
G. Dujany[56], K. Dungs[40], P. Durante[40], R. Dzhelyadin[37], A. Dziurda[40], A. Dzyuba[31],
N. Déléage[4], S. Easo[51], M. Ebert[52], U. Egede[55], V. Egorychev[32], S. Eidelman[36,w],
S. Eisenhardt[52], U. Eitschberger[10], R. Ekelhof[10], L. Eklund[53], S. Ely[61], S. Esen[12], H.M. Evans[49],
T. Evans[57], A. Falabella[15], N. Farley[47], S. Farry[54], R. Fay[54], D. Fazzini[21,i], D. Ferguson[52],
A. Fernandez Prieto[39], F. Ferrari[15,40], F. Ferreira Rodrigues[2], M. Ferro-Luzzi[40], S. Filippov[34],
R.A. Fini[14], M. Fiore[17,g], M. Fiorini[17,g], M. Firlej[28], C. Fitzpatrick[41], T. Fiutowski[28],
F. Fleuret[7,b], K. Fohl[40], M. Fontana[16,40], F. Fontanelli[20,h], D.C. Forshaw[61], R. Forty[40],
V. Franco Lima[54], M. Frank[40], C. Frei[40], J. Fu[22,q], E. Furfaro[25,j], C. Färber[40],
A. Gallas Torreira[39], D. Galli[15,e], S. Gallorini[23], S. Gambetta[52], M. Gandelman[2], P. Gandini[57],
Y. Gao[3], L.M. Garcia Martin[69], J. García Pardiñas[39], J. Garra Tico[49], L. Garrido[38],
P.J. Garsed[49], D. Gascon[38], C. Gaspar[40], L. Gavardi[10], G. Gazzoni[5], D. Gerick[12], E. Gersabeck[12],
M. Gersabeck[56], T. Gershon[50], Ph. Ghez[4], S. Gianì[41], V. Gibson[49], O.G. Girard[41], L. Giubega[30],
K. Gizdov[52], V.V. Gligorov[8], D. Golubkov[32], A. Golutvin[55,40], A. Gomes[1,a], I.V. Gorelov[33],
C. Gotti[21,i], M. Grabalosa Gándara[5], R. Graciani Diaz[38], L.A. Granado Cardoso[40], E. Graugés[38],

JHEP03 (2017) 001

– 14 –

E. Graverini[42], G. Graziani[18], A. Grecu[30], P. Griffith[47], L. Grillo[21,40,i], B.R. Gruberg Cazon[57],
O. Grünberg[67], E. Gushchin[34], Yu. Guz[37], T. Gys[40], C. Göbel[62], T. Hadavizadeh[57],
C. Hadjivasiliou[5], G. Haefeli[41], C. Haen[40], S.C. Haines[49], S. Hall[55], B. Hamilton[60], X. Han[12],
S. Hansmann-Menzemer[12], N. Harnew[57], S.T. Harnew[48], J. Harrison[56], M. Hatch[40], J. He[63],
T. Head[41], A. Heister[9], K. Hennessy[54], P. Henrard[5], L. Henry[8], J.A. Hernando Morata[39],
E. van Herwijnen[40], M. Heß[67], A. Hicheur[2], D. Hill[57], C. Hombach[56], H. Hopchev[41],
W. Hulsbergen[43], T. Humair[55], M. Hushchyn[35], N. Hussain[57], D. Hutchcroft[54], M. Idzik[28],
P. Ilten[58], R. Jacobsson[40], A. Jaeger[12], J. Jalocha[57], E. Jans[43], A. Jawahery[60], F. Jiang[3],
M. John[57], D. Johnson[40], C.R. Jones[49], C. Joram[40], B. Jost[40], N. Jurik[61], S. Kandybei[45],
W. Kanso[6], M. Karacson[40], J.M. Kariuki[48], S. Karodia[53], M. Kecke[12], M. Kelsey[61],
I.R. Kenyon[47], M. Kenzie[49], T. Ketel[44], E. Khairullin[35], B. Khanji[12], C. Khurewathanakul[41],
T. Kirn[9], S. Klaver[56], K. Klimaszewski[29], S. Koliiev[46], M. Kolpin[12], I. Komarov[41],
R.F. Koopman[44], P. Koppenburg[43], A. Kosmyntseva[32], A. Kozachuk[33], M. Kozeiha[5],
L. Kravchuk[34], K. Kreplin[12], M. Kreps[50], P. Krokovny[36,w], F. Kruse[10], W. Krzemien[29],
W. Kucewicz[27,l], M. Kucharczyk[27], V. Kudryavtsev[36,w], A.K. Kuonen[41], K. Kurek[29],
T. Kvaratskheliya[32,40], D. Lacarrere[40], G. Lafferty[56], A. Lai[16], G. Lanfranchi[19], C. Langenbruch[9],
T. Latham[50], C. Lazzeroni[47], R. Le Gac[6], J. van Leerdam[43], J.-P. Lees[4], A. Leflat[33,40],
J. Lefrançois[7], R. Lefèvre[5], F. Lemaitre[40], E. Lemos Cid[39], O. Leroy[6], T. Lesiak[27],
B. Leverington[12], Y. Li[7], T. Likhomanenko[35,68], R. Lindner[40], C. Linn[40], F. Lionetto[42], B. Liu[16],
X. Liu[3], D. Loh[50], I. Longstaff[53], J.H. Lopes[2], D. Lucchesi[23,o], M. Lucio Martinez[39], H. Luo[52],
A. Lupato[23], E. Luppi[17,g], O. Lupton[57], A. Lusiani[24], X. Lyu[63], F. Machefert[7], F. Maciuc[30],
O. Maev[31], K. Maguire[56], S. Malde[57], A. Malinin[68], T. Maltsev[36], G. Manca[7], G. Mancinelli[6],
P. Manning[61], J. Maratas[5,v], J.F. Marchand[4], U. Marconi[15], C. Marin Benito[38], P. Marino[24,t],
J. Marks[12], G. Martellotti[26], M. Martin[6], M. Martinelli[41], D. Martinez Santos[39],
F. Martinez Vidal[69], D. Martins Tostes[2], L.M. Massacrier[7], A. Massafferri[1], R. Matev[40],
A. Mathad[50], Z. Mathe[40], C. Matteuzzi[21], A. Mauri[42], B. Maurin[41], A. Mazurov[47],
M. McCann[55], J. McCarthy[47], A. McNab[56], R. McNulty[13], B. Meadows[59], F. Meier[10],
M. Meissner[12], D. Melnychuk[29], M. Merk[43], A. Merli[22,q], E. Michielin[23], D.A. Milanes[66],
M.-N. Minard[4], D.S. Mitzel[12], A. Mogini[8], J. Molina Rodriguez[1], I.A. Monroy[66], S. Monteil[5],
M. Morandin[23], P. Morawski[28], A. Mordà[6], M.J. Morello[24,t], J. Moron[28], A.B. Morris[52],
R. Mountain[61], F. Muheim[52], M. Mulder[43], M. Mussini[15], D. Müller[56], J. Müller[10], K. Müller[42],
V. Müller[10], P. Naik[48], T. Nakada[41], R. Nandakumar[51], A. Nandi[57], I. Nasteva[2], M. Needham[52],
N. Neri[22], S. Neubert[12], N. Neufeld[40], M. Neuner[12], A.D. Nguyen[41], T.D. Nguyen[41],
C. Nguyen-Mau[41,n], S. Nieswand[9], R. Niet[10], N. Nikitin[33], T. Nikodem[12], A. Novoselov[37],
D.P. O'Hanlon[50], A. Oblakowska-Mucha[28], V. Obraztsov[37], S. Ogilvy[19], R. Oldeman[49],
C.J.G. Onderwater[70], J.M. Otalora Goicochea[2], A. Otto[40], P. Owen[42], A. Oyanguren[69,40],
P.R. Pais[41], A. Palano[14,d], F. Palombo[22,q], M. Palutan[19], J. Panman[40], A. Papanestis[51],
M. Pappagallo[14,d], L.L. Pappalardo[17,g], W. Parker[60], C. Parkes[56], G. Passaleva[18], A. Pastore[14,d],
G.D. Patel[54], M. Patel[55], C. Patrignani[15,e], A. Pearce[56,51], A. Pellegrino[43], G. Penso[26],
M. Pepe Altarelli[40], S. Perazzini[40], P. Perret[5], L. Pescatore[47], K. Petridis[48], A. Petrolini[20,h],
A. Petrov[68], M. Petruzzo[22,q], E. Picatoste Olloqui[38], B. Pietrzyk[4], M. Pikies[27], D. Pinci[26],
A. Pistone[20], A. Piucci[12], S. Playfer[52], M. Plo Casasus[39], T. Poikela[40], F. Polci[8],
A. Poluektov[50,36], I. Polyakov[61], E. Polycarpo[2], G.J. Pomery[48], A. Popov[37], D. Popov[11,40],
B. Popovici[30], S. Poslavskii[37], C. Potterat[2], E. Price[48], J.D. Price[54], J. Prisciandaro[39],
A. Pritchard[54], C. Prouve[48], V. Pugatch[46], A. Puig Navarro[41], G. Punzi[24,p], W. Qian[57],
R. Quagliani[7,48], B. Rachwal[27], J.H. Rademacker[48], M. Rama[24], M. Ramos Pernas[39],
M.S. Rangel[2], I. Raniuk[45], F. Ratnikov[35], G. Raven[44], F. Redi[55], S. Reichert[10], A.C. dos Reis[1],
C. Remon Alepuz[69], V. Renaudin[7], S. Ricciardi[51], S. Richards[48], M. Rihl[40], K. Rinnert[54],

V. Rives Molina[38], P. Robbe[7,40], A.B. Rodrigues[1], E. Rodrigues[59], J.A. Rodriguez Lopez[66],
P. Rodriguez Perez[56,†], A. Rogozhnikov[35], S. Roiser[40], A. Rollings[57], V. Romanovskiy[37],
A. Romero Vidal[39], J.W. Ronayne[13], M. Rotondo[19], M.S. Rudolph[61], T. Ruf[40], P. Ruiz Valls[69],
J.J. Saborido Silva[39], E. Sadykhov[32], N. Sagidova[31], B. Saitta[16,f], V. Salustino Guimaraes[2],
C. Sanchez Mayordomo[69], B. Sanmartin Sedes[39], R. Santacesaria[26], C. Santamarina Rios[39],
M. Santimaria[19], E. Santovetti[25,j], A. Sarti[19,k], C. Satriano[26,s], A. Satta[25], D.M. Saunders[48],
D. Savrina[32,33], S. Schael[9], M. Schellenberg[10], M. Schiller[40], H. Schindler[40], M. Schlupp[10],
M. Schmelling[11], T. Schmelzer[10], B. Schmidt[40], O. Schneider[41], A. Schopper[40], K. Schubert[10],
M. Schubiger[41], M.-H. Schune[7], R. Schwemmer[40], B. Sciascia[19], A. Sciubba[26,k], A. Semennikov[32],
A. Sergi[47], N. Serra[42], J. Serrano[6], L. Sestini[23], P. Seyfert[21], M. Shapkin[37], I. Shapoval[45],
Y. Shcheglov[31], T. Shears[54], L. Shekhtman[36,w], V. Shevchenko[68], B.G. Siddi[17,40],
R. Silva Coutinho[42], L. Silva de Oliveira[2], G. Simi[23,o], S. Simone[14,d], M. Sirendi[49], N. Skidmore[48],
T. Skwarnicki[61], E. Smith[55], I.T. Smith[52], J. Smith[49], M. Smith[55], H. Snoek[43], M.D. Sokoloff[59],
F.J.P. Soler[53], B. Souza De Paula[2], B. Spaan[10], P. Spradlin[53], S. Sridharan[40], F. Stagni[40],
M. Stahl[12], S. Stahl[40], P. Stefko[41], S. Stefkova[55], O. Steinkamp[42], S. Stemmle[12], O. Stenyakin[37],
S. Stevenson[57], S. Stoica[30], S. Stone[61], B. Storaci[42], S. Stracka[24,p], M. Straticiuc[30],
U. Straumann[42], L. Sun[64], W. Sutcliffe[55], K. Swientek[28], V. Syropoulos[44], M. Szczekowski[29],
T. Szumlak[28], S. T'Jampens[4], A. Tayduganov[6], T. Tekampe[10], M. Teklishyn[7], G. Tellarini[17,g],
F. Teubert[40], E. Thomas[40], J. van Tilburg[43], M.J. Tilley[55], V. Tisserand[4], M. Tobin[41], S. Tolk[49],
L. Tomassetti[17,g], D. Tonelli[40], S. Topp-Joergensen[57], F. Toriello[61], E. Tournefier[4], S. Tourneur[41],
K. Trabelsi[41], M. Traill[53], M.T. Tran[41], M. Tresch[42], A. Trisovic[40], A. Tsaregorodtsev[6],
P. Tsopelas[43], A. Tully[49], N. Tuning[43], A. Ukleja[29], A. Ustyuzhanin[35,x], U. Uwer[12], C. Vacca[16,f],
V. Vagnoni[15,40], A. Valassi[40], S. Valat[40], G. Valenti[15], A. Vallier[7], R. Vazquez Gomez[19],
P. Vazquez Regueiro[39], S. Vecchi[17], M. van Veghel[43], J.J. Velthuis[48], M. Veltri[18,r],
G. Veneziano[57], A. Venkateswaran[61], M. Vernet[5], M. Vesterinen[12], B. Viaud[7], D. Vieira[1],
M. Vieites Diaz[39], H. Viemann[67], X. Vilasis-Cardona[38,m], M. Vitti[49], V. Volkov[33], A. Vollhardt[42],
B. Voneki[40], A. Vorobyev[31], V. Vorobyev[36,w], C. Voß[67], J.A. de Vries[43], C. Vázquez Sierra[39],
R. Waldi[67], C. Wallace[50], R. Wallace[13], J. Walsh[24], J. Wang[61], D.R. Ward[49], H.M. Wark[54],
N.K. Watson[47], D. Websdale[55], A. Weiden[42], M. Whitehead[40], J. Wicht[50], G. Wilkinson[57,40],
M. Wilkinson[61], M. Williams[40], M.P. Williams[47], M. Williams[58], T. Williams[47], F.F. Wilson[51],
J. Wimberley[60], J. Wishahi[10], W. Wislicki[29], M. Witek[27], G. Wormser[7], S.A. Wotton[49],
K. Wraight[53], K. Wyllie[40], Y. Xie[65], Z. Xing[61], Z. Xu[41], Z. Yang[3], Y. Yao[61], H. Yin[65], J. Yu[65],
X. Yuan[36,w], O. Yushchenko[37], K.A. Zarebski[47], M. Zavertyaev[11,c], L. Zhang[3], Y. Zhang[7],
Y. Zhang[63], A. Zhelezov[12], Y. Zheng[63], A. Zhokhov[32], X. Zhu[3], V. Zhukov[9], S. Zucchelli[15]

1   *Centro Brasileiro de Pesquisas Físicas (CBPF), Rio de Janeiro, Brazil*
2   *Universidade Federal do Rio de Janeiro (UFRJ), Rio de Janeiro, Brazil*
3   *Center for High Energy Physics, Tsinghua University, Beijing, China*
4   *LAPP, Université Savoie Mont-Blanc, CNRS/IN2P3, Annecy-Le-Vieux, France*
5   *Clermont Université, Université Blaise Pascal, CNRS/IN2P3, LPC, Clermont-Ferrand, France*
6   *CPPM, Aix-Marseille Université, CNRS/IN2P3, Marseille, France*
7   *LAL, Université Paris-Sud, CNRS/IN2P3, Orsay, France*
8   *LPNHE, Université Pierre et Marie Curie, Université Paris Diderot, CNRS/IN2P3, Paris, France*
9   *I. Physikalisches Institut, RWTH Aachen University, Aachen, Germany*
10 *Fakultät Physik, Technische Universität Dortmund, Dortmund, Germany*
11 *Max-Planck-Institut für Kernphysik (MPIK), Heidelberg, Germany*
12 *Physikalisches Institut, Ruprecht-Karls-Universität Heidelberg, Heidelberg, Germany*
13 *School of Physics, University College Dublin, Dublin, Ireland*
14 *Sezione INFN di Bari, Bari, Italy*

15 *Sezione INFN di Bologna, Bologna, Italy*
16 *Sezione INFN di Cagliari, Cagliari, Italy*
17 *Sezione INFN di Ferrara, Ferrara, Italy*
18 *Sezione INFN di Firenze, Firenze, Italy*
19 *Laboratori Nazionali dell'INFN di Frascati, Frascati, Italy*
20 *Sezione INFN di Genova, Genova, Italy*
21 *Sezione INFN di Milano Bicocca, Milano, Italy*
22 *Sezione INFN di Milano, Milano, Italy*
23 *Sezione INFN di Padova, Padova, Italy*
24 *Sezione INFN di Pisa, Pisa, Italy*
25 *Sezione INFN di Roma Tor Vergata, Roma, Italy*
26 *Sezione INFN di Roma La Sapienza, Roma, Italy*
27 *Henryk Niewodniczanski Institute of Nuclear Physics Polish Academy of Sciences, Kraków, Poland*
28 *AGH — University of Science and Technology, Faculty of Physics and Applied Computer Science, Kraków, Poland*
29 *National Center for Nuclear Research (NCBJ), Warsaw, Poland*
30 *Horia Hulubei National Institute of Physics and Nuclear Engineering, Bucharest-Magurele, Romania*
31 *Petersburg Nuclear Physics Institute (PNPI), Gatchina, Russia*
32 *Institute of Theoretical and Experimental Physics (ITEP), Moscow, Russia*
33 *Institute of Nuclear Physics, Moscow State University (SINP MSU), Moscow, Russia*
34 *Institute for Nuclear Research of the Russian Academy of Sciences (INR RAN), Moscow, Russia*
35 *Yandex School of Data Analysis, Moscow, Russia*
36 *Budker Institute of Nuclear Physics (SB RAS), Novosibirsk, Russia*
37 *Institute for High Energy Physics (IHEP), Protvino, Russia*
38 *ICCUB, Universitat de Barcelona, Barcelona, Spain*
39 *Universidad de Santiago de Compostela, Santiago de Compostela, Spain*
40 *European Organization for Nuclear Research (CERN), Geneva, Switzerland*
41 *Insitute of Physics, Ecole Polytechnique Fédérale de Lausanne (EPFL), Lausanne, Switzerland*
42 *Physik-Institut, Universität Zürich, Zürich, Switzerland*
43 *Nikhef National Institute for Subatomic Physics, Amsterdam, The Netherlands*
44 *Nikhef National Institute for Subatomic Physics and VU University Amsterdam, Amsterdam, The Netherlands*
45 *NSC Kharkiv Institute of Physics and Technology (NSC KIPT), Kharkiv, Ukraine*
46 *Institute for Nuclear Research of the National Academy of Sciences (KINR), Kyiv, Ukraine*
47 *University of Birmingham, Birmingham, United Kingdom*
48 *H.H. Wills Physics Laboratory, University of Bristol, Bristol, United Kingdom*
49 *Cavendish Laboratory, University of Cambridge, Cambridge, United Kingdom*
50 *Department of Physics, University of Warwick, Coventry, United Kingdom*
51 *STFC Rutherford Appleton Laboratory, Didcot, United Kingdom*
52 *School of Physics and Astronomy, University of Edinburgh, Edinburgh, United Kingdom*
53 *School of Physics and Astronomy, University of Glasgow, Glasgow, United Kingdom*
54 *Oliver Lodge Laboratory, University of Liverpool, Liverpool, United Kingdom*
55 *Imperial College London, London, United Kingdom*
56 *School of Physics and Astronomy, University of Manchester, Manchester, United Kingdom*
57 *Department of Physics, University of Oxford, Oxford, United Kingdom*
58 *Massachusetts Institute of Technology, Cambridge, MA, United States*
59 *University of Cincinnati, Cincinnati, OH, United States*
60 *University of Maryland, College Park, MD, United States*
61 *Syracuse University, Syracuse, NY, United States*
62 *Pontifícia Universidade Católica do Rio de Janeiro (PUC-Rio), Rio de Janeiro, Brazil, associated to[2]*

[63] *University of Chinese Academy of Sciences, Beijing, China, associated to* [3]

[64] *School of Physics and Technology, Wuhan University, Wuhan, China, associated to* [3]

[65] *Institute of Particle Physics, Central China Normal University, Wuhan, Hubei, China, associated to* [3]

[66] *Departamento de Fisica , Universidad Nacional de Colombia, Bogota, Colombia, associated to* [8]

[67] *Institut für Physik, Universität Rostock, Rostock, Germany, associated to* [12]

[68] *National Research Centre Kurchatov Institute, Moscow, Russia, associated to* [32]

[69] *Instituto de Fisica Corpuscular (IFIC), Universitat de Valencia-CSIC, Valencia, Spain, associated to* [38]

[70] *Van Swinderen Institute, University of Groningen, Groningen, The Netherlands, associated to* [43]

[a] *Universidade Federal do Triângulo Mineiro (UFTM), Uberaba-MG, Brazil*

[b] *Laboratoire Leprince-Ringuet, Palaiseau, France*

[c] *P.N. Lebedev Physical Institute, Russian Academy of Science (LPI RAS), Moscow, Russia*

[d] *Università di Bari, Bari, Italy*

[e] *Università di Bologna, Bologna, Italy*

[f] *Università di Cagliari, Cagliari, Italy*

[g] *Università di Ferrara, Ferrara, Italy*

[h] *Università di Genova, Genova, Italy*

[i] *Università di Milano Bicocca, Milano, Italy*

[j] *Università di Roma Tor Vergata, Roma, Italy*

[k] *Università di Roma La Sapienza, Roma, Italy*

[l] *AGH — University of Science and Technology, Faculty of Computer Science, Electronics and Telecommunications, Kraków, Poland*

[m] *LIFAELS, La Salle, Universitat Ramon Llull, Barcelona, Spain*

[n] *Hanoi University of Science, Hanoi, Viet Nam*

[o] *Università di Padova, Padova, Italy*

[p] *Università di Pisa, Pisa, Italy*

[q] *Università degli Studi di Milano, Milano, Italy*

[r] *Università di Urbino, Urbino, Italy*

[s] *Università della Basilicata, Potenza, Italy*

[t] *Scuola Normale Superiore, Pisa, Italy*

[u] *Università di Modena e Reggio Emilia, Modena, Italy*

[v] *Iligan Institute of Technology (IIT), Iligan, Philippines*

[w] *Novosibirsk State University, Novosibirsk, Russia*

[x] *Moscow Institute of Physics and Technology, Moscow, Russia* [†] *Deceased*